

DESIGN AND CONTROL OF HYBRID ENERGY STORAGE SYSTEM FOR DC GRID VOLTAGE REGULATION

Byroju Srinath¹ Jarupula Srinivas² T Siva balaji*

1. Byroju Srinath, Asst. Professor, EEE Department, Sri Indu college of Engineering and Technology

2. J Srinivas, Asst. Professor EEE Department, Sri Indhu college of Engineering and Technology

*Corresponding Author, Asst. Professor, EEE Dept, Gurunanak Institutions Technical Campus, Hyd, T.S

ABSTRACT: The present paper deals with development of new control strategy for hybrid energy storage system (HESS), consisting of photovoltaic (PV) system, battery, Supercapacitor (SC) and load. Due to the variable characteristics of nonconventional power generation and variable load demand, batteries can undergo irregular, partial charge/discharge cycles. It has detrimental effects on battery life span and rating.

The proposed strategy uses the DC bus voltage and battery state of charge (SOC) for charging/discharging of battery. In the proposed method, the battery system is coordinated with SC by diverting short-term charge/discharge cycles to SC if the SOC is within the limits. In case of SOC limit violation, battery SOC is controlled by diverting charge/discharge currents to SC. The digital simulation results are presented and discussed to verify the validity of the proposed control strategy.

I. INTRODUCTION

Renewable source is currently considered as one of the most useful energy source. In remote areas where connection to the main utility grid is not feasible, standalone renewable generation can offer the benefit of reduced running and maintenance costs. Due to the variable nature of PV power and load demand, a PV system alone cannot supply the load demand. At present, battery storage systems seems to provide a promising opportunity to mitigate the issues of load demand and power generation fluctuations in most real life remote area power system (RAPS) applications.

	Lead acid battery	Super-capacitor
Specific energy density	10-100 (Wh/kg)	1-10 (Wh/kg)
Specific power density	< 1000 (W/kg)	< 10000 (W/kg)
Cycle life	1000	> 500000
Charge/ discharge efficiency	70-85%	85-98%
Fast charge time	1-5 hr	03-30 sec
Discharge time	0.3-3 hr	0.3-30 sec

Table.1: Battery versus Supercapacitor Performance

The typical energy storage applied in standalone PV system is lead acid batteries. Batteries have high energy density but low power density, low charge/discharge rates. The Supercapacitors (SC) are new form of energy storage which stores energy by means of static charge. When compared to batteries, SC possess high power density but low energy density, high charge/discharge rates. In Table I the battery and the Supercapacitor performance are compared.

Fig. 1 shows the energy density and power density profiles of different energy storages, whereas a general theory of Ragone plot is provided. The battery area is an average of the most common battery types such as Li-Ion and NiMH. If we use only battery as storage, then it has to be oversized to take care of the peak load demand. An ideal energy storage system (ESS) in a standalone PV system should be able to provide both high energy and power capacities to handle situations such as weather changes and load step changes. Thus, the objective is to harness the advantages of both batteries and SCs to design ESS with high power and energy density.

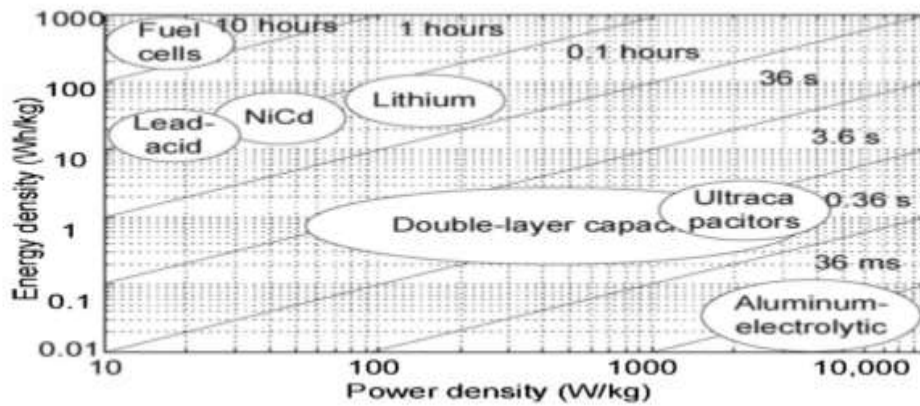


Fig. 1 Ragone chart

By utilizing a battery Supercapacitor hybrid energy storage system (HESS) the following advantages can be achieved: i) improvement in battery life span ii) reduction in battery size and hence the cost iii) reduction in stress on battery and iv) improvement in power balance between power generation and load.

Batteries and super capacitors are combined together for better performance. In the fig 2(a) battery and super capacitor combination is directly connected to a load bus such that it does not have an control on the battery, super capacitor and load voltage. The load voltage of such configurations is uncontrolled and follows the battery charge/discharge curve. In the fig 2(a), this configuration can control the load voltage by regulating the dc/dc converter. But by this configuration it cannot have power sharing between batteries and super capacitors. In the fig 2(b-d), one or more controlled energy storage units are present. In these configurations, dc/dc converters are placed between energy storage elements and load. These converters are used to control the power between the energy storage units and load, thereby enhancing the power capability among the actively controlled configurations, fig. 2(b-d) provides active control of energy storage devices, one at a time. The configuration shown in fig. 2(d) it has a capability to control independently on both battery and the super capacitors.

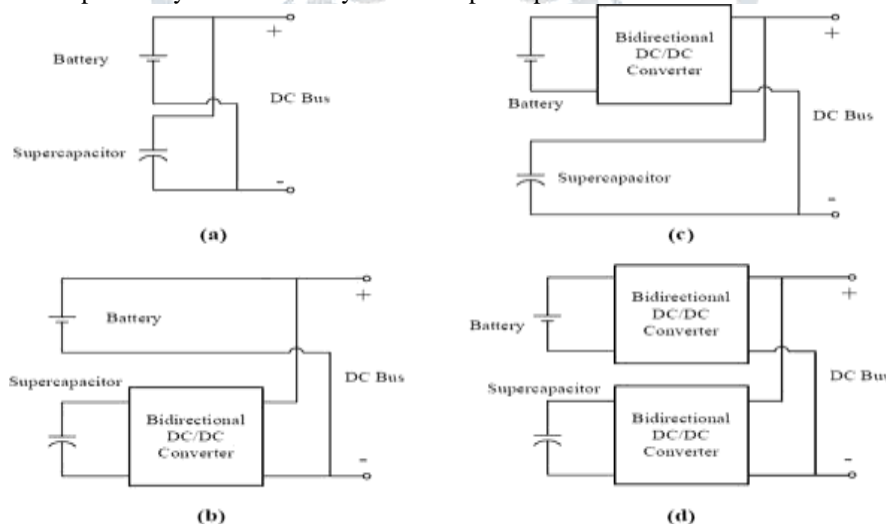


Fig. 2 Different Configurations of Battery-Supercapacitor HESS

In this paper we have considered the same kind of configuration. In practical energy storage applications, battery cells or super capacitor cells are connected in series to meet the load demands. In general cell imbalances occur among series connected battery and super capacitor cells due to inevitable chemical and electrical operational conditions. Several cell balancing circuits are reported in literature to balance the voltages between cells.

By using super capacitors in hybrid energy storage systems can reduce the stress level on the battery. This demonstrates that by hybrid energy storage system can improve its efficiency and also reduces the cost of the battery. In this paper several control schemes have been reported to control HESS. Most of them are related to real time appliances like hybrid electric vehicle. But there are only few applications which depend on dc grid voltage regulation. The DC grid sources like wind, PV, batteries and SC which has both DC and AC busses were focused on control strategies of a micro grid. The authors were mainly concentrated on the on the controlling the state of charge of different batteries by using different switches and control of hysteresis. This has presented a simple control strategy to organize the power between renewable power sources and storage systems, but this scheme did not consider the power shared between storage systems internally. Similar to the above scheme the control strategy proposed in lack of clarity of current control between the HESS i.e., battery and Supercapacitor to handle the fluctuations in the power demands. The proposed scheme of a composite converter for HESS in a distributed renewable energy generating system. But this scheme did not concentrate on grid voltage regulation during power fluctuations.

Fengyan Zhang *et al.* proposed a power management scheme to control the power in dc microgrid. In this the voltage has been categorized into seven ranges, each can be operated accordingly. At transient conditions, the dc grid voltage fails to maintain the desired voltage level. However new control schemes are proposed in those schemes priority based algorithm is designed to

coordinate the power between Hess and the renewable energy source. In this new scheme the algorithm was designed in such a way that super capacitor is placed at a higher priority than that of battery storage system.

The low frequency power components are passed to the battery and the remaining power components were diverted to super capacitor to undergo this process power filter based control approach for wind power applications has been proposed. In this case detailed explanation about the design of power filter has not provided.

The reference idea from all the modes of control scheme is that super capacitor will take care of control scheme is that super capacitor will take care of high frequency power component and where as battery will take care of average power component, but some of the control schemes were not considered about the dc grid voltage regulation during poor fluctuations. As explained if the battery tries to operate with high power the battery tends to premature failure. Therefore it is important to control the stress level on the battery then the life span of the battery increases.

In this paper, a new control strategy is proposed for Hess to control the grid voltage and charge/discharge rate of the battery. The performance of the Hess basically depends on three parameters a) the maximum allowable charge/discharge rate of battery, b) the battery converter response time and c) the control strategy. This is because the super capacitor has a high power density compared to that of battery. With this scheme, the Hess performance is improved without changing the converter components.

Different control strategies have been reported in literature, for controlling power sharing between battery and Supercapacitor. N. Mendis et al. has addressed the benefits of adding a SC to a battery storage system in a wind based hybrid RAPS system. In this regard, an energy management algorithm (EMA) has been established between the battery storage system and SC to operate both energy storage systems in a designated manner. Authors in [7] have proposed HESS for microgrid applications. Amine Lahyani et al. [12] presented a study of the reduction in battery stresses by using Sc. Authors in [13], demonstrated that HESS lowers the battery cost and improves the overall system efficiency. The fundamental idea of all these control strategies is that battery provides low frequency power component and SC provides high frequency power component momentarily. In this paper, a new control strategy is proposed for HESS consisting of PV, battery, SC and load. The proposed method is based on decoupling of low and high frequency power components and utilizes SOC of battery to control the SC.

II. SYSTEM CONFIGURATION OF REMOTE AREA POWER SYSTEMS

Fig. 3 shows the typical configuration of standalone RAPS. The system consists of the PV panel, wind turbine, diesel set, battery, SC and power electronic converters. To demonstrate the proposed control strategy, PV or any other renewable energy source is represented by an equivalent DC power generation connected to the DC grid using a DC-DC converter as shown in Fig. 4. Further, DC and AC loads are represented with an equivalent DC load resistance R connected to the DC grid. Batteries and SCs are connected to the DC grid to form HESS using a bidirectional buck-boost converter. Here, the hybrid energy storage system is used to regulate the DC grid voltage (V_0) and compensate the power imbalances in the system. When the power generation is less than the load demand, then there will be decrease in the DC grid voltage.

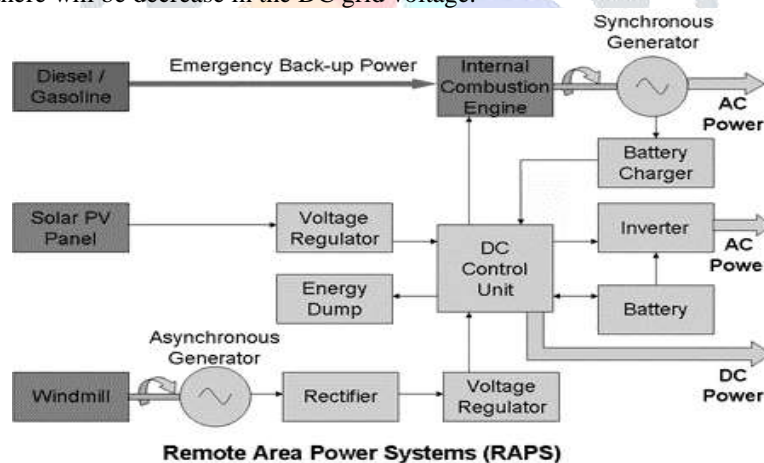


Fig. 3 Standalone Configuration of Remote Area Power Systems (RAPS)

Therefore, to compensate the power deficiency, the HESS supplies the surplus power demand. Similarly, when the power generation is more than load demand, then there will be increase in DC grid voltage. Therefore, to regulate the grid voltage, the HESS will absorb the surplus power generation.

A standalone PV system consisting of PV panel, battery and SC arrangement is shown in Fig.4. The PV panel is connected to DC grid using a boost converter. Here, the boost converter is used to extract the maximum power from PV panel using maximum power point tracking (MPPT) algorithm. HESS is connected to DC grid using bi-directional DCIDC converter. HESS is used to maintain the constant DC grid voltage (V_0) due to mismatch between generation and demand. When the demand is more than generation, V_0 drops from its reference value, consequently HESS will discharge to provide the surplus demand.

Similarly, when the demand is less than generation, V_0 increases from its reference value, consequently HESS will charge to absorb the surplus power. Buck-boost converter is used as a bi-directional converter to facilitate the bi-directional power flow between DC grid and HESS.

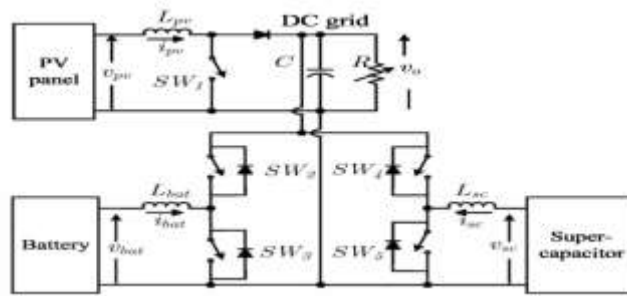


Fig. 4 Configuration of PV based DC grid

In this paper, the total load is represented as DC load with resistance R. In Fig. 2 V_{pv} , V_{batt} and V_{sc} are PV panel, battery and SC voltages respectively, i_{pv} , i_{batt} and i_{sc} are PV panel, battery and SC current respectively, L_{pv} , L_{bat} and L_{sc} are PV panel, battery and SC filter inductance respectively, V_0 is DC grid voltage, C is filter capacitance and R is load resistance. SW_1 , SW_2 , SW_3 , SW_4 and SW_5 are control switches.

A. Modelling of PV Module

The photovoltaic (PV) cell is basically a p-n junction fabricated in a thin wafer of semiconductor. The solar energy is directly converted to electricity through photovoltaic effect. PV cell exhibits a nonlinear P-V and I-V characteristics which vary with cell temperature (T) and solar irradiance (S). The nonlinear voltage-current characteristic equation of PV module is given as,

$$I_{pv} = N_p I_{ph} - N_p I_{rs} \left(e^{\frac{q(V_{pv}/N_s + I_{pv} R_s)/kT}{A}} - 1 \right) - \frac{N_p V_{pv}/N_s + I_{pv} R_s}{R_{sh}} \quad (1)$$

where I_{pv} is terminal current (A), I_{ph} is light generated current or photo current (A), I_{rs} is diode reverse saturation current, V_{pv} is terminal voltage (V), q is electron charge(= $1.609 \times 10^{-19} C$), A is diode ideality constant, k is Boltzmann's constant (= $1.38 \times 10^{-23} J/K$), T is cell absolute temperature (K), N_p is number of cells in parallel, N_s is number of cells in series and other parameters can be obtained from specifications.

B. Modelling of Battery

The battery is modelled using a simple controlled voltage source in series with a constant resistance. The battery is modelled as a nonlinear voltage source using the following equations,

$$E = E_0 - K \frac{Q}{Q - \int i dt} + A e^{-B \int i dt} \quad (2)$$

$$V_{batt} = E - Ri \quad (3)$$

$$\%SOC = \left(1 - \frac{1}{Q} \int i dt \right) * 100 \quad (4)$$

where i and V_{batt} are terminal current and voltage of battery, and other parameters can be obtained from specifications.

C. Modelling of Supercapacitor

The SC is an emerging technology in the field of energystorage systems. The SC resembles a regular capacitor with the exception that it offers very high capacitance in a small package. Energy storage is by means of static charge rather than of an electrochemical process that is inherent to the battery. The three branch model of Supercapacitor is shown in Fig. 5. The C_1 is the main capacitance responsible for energy storage and charge handling. The R_1 accounts for self discharge effect and ESR are added to include the losses during charging and discharging. The R_F and C_F are responsible for the fast dynamic behaviour of SCs. Procedure to determine the parameters are discussed.

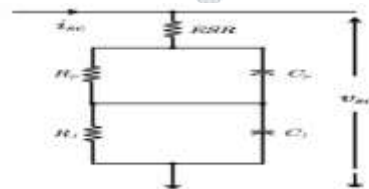


Fig. 5 Equivalent Circuit of Supercapacitor

III. NEW CONTROL STRATEGY FOR CONTROLLINGESS

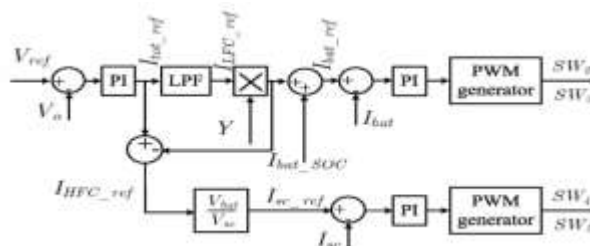


Fig. 6 Block Diagram of Battery Supercapacitor controller

Fig. 6 shows the block diagram of the proposed control strategy. In this algorithm the DC grid voltage (V_0) is compared with reference voltage (V_{ref}), and the error is given to the proportional-integral (PI) controller. The PI controller generates the total current required (I_{tot_ref}) from energy storage system. I_{tot_ref} is divided into low frequency component (I_{LFC_ref}) and high frequency component (I_{HFC_ref}) as

$$I_{LFC_ref} = \text{lowpassfilter}(I_{tot_ref}) \quad (5)$$

$$I_{HFC_ref} = I_{tot_ref} - I_{LFC_ref} * Y \quad (6)$$

where Y is the output of SOC control loop as shown in Fig. 5. The low frequency component along with output of SOC control loop (Y, I_{bat_SOC}), gives the reference current to battery as given

$$I_{bat_ref} = I_{LFC_ref} * Y + I_{bat_SOC} \quad (7)$$

I_{bat_ref} is compared with the actual battery current (I_{bat}), and the error is given to the PI controller. The PI controller generates the duty ratios (D_2, D_3). These duty ratios are given to the PWM generator to generate switching pulses corresponding to battery switches (SW_2, SW_3).

The high frequency component is compensated by SC. Therefore, the reference current of SC is given as

$$I_{sc_ref} = I_{HFC_ref} * \frac{V_{bat}}{V_{sc}} \quad (8)$$

I_{sc_ref} is compared with the actual SC current (I_{sc}), and the error is given to the PI controller. The PI controller generates the duty ratios (D_4, D_5) These duty ratios are given to the PWM generator to generate switching pulses corresponding to SC switches (SW_4, SW_5).

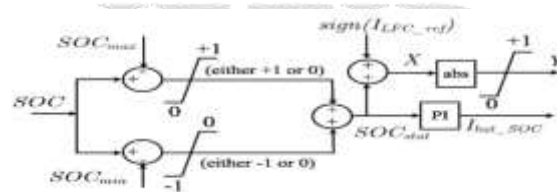


Fig. 7 Block Diagram of SOC controller

Fig. 7 shows the block diagram of SOC control loop. In this controller, SOC is compared with SOC_{max} and SOC_{min} . The errors corresponding to SOC_{max} and SOC_{min} are limited to (+1 or 0), and (-1 or 0) respectively. These errors are added to get the status of the state of charge (SOC_{stat}) as given

$$SOC_{stat} = \begin{cases} -1 & \text{if } SOC < SOC_{min} \\ 0 & \text{if } SOC_{max} \geq SOC \geq SOC_{min} \\ +1 & \text{if } SOC > SOC_{max} \end{cases} \quad (9)$$

SOC_{stat} is given to the PI controller. The PI controller generates the additional charge/discharge battery current (I_{bat_SOC}), required to maintain the battery SOC within the limits.

IV. SIMULATION RESULTS

The proposed control strategy is verified for the following cases: i) step decrease in PV generation ii) step increase in PV generation iii) step decrease in load demand and iv) step increase in load demand. The objective is to maintain the DC grid voltage at $V_{ref} = 48$ V. The nominal parameters of the DC grid are given in Table III. The initial SOC of the battery is set at 50%. To verify the proposed strategy it is assumed that $SOC_{max} = 50.5\%$ and

$SOC_{min} = 49.5\%$. The PI controller gains of the outer voltage loop, inner current loop of battery, inner current loop of SC and SOC control loop are $Kp_v = 10477$, $Ki_v = 3077$, $Kp_{bat} = 0.05$, $Ki_{bat} = 305$, $Kp_{sc} = 0.04$, $Ki_{sc} = 14393$, $Kp_{soc} = 0.5$ and $Ki_{soc} = 1$.

A. Case 1: Step Decrease in PV Generation

In this study, initially the PV panel is operated in maximum power point tracking (MPPT) mode with $S = 520$ W/m² and $T = 25^\circ\text{C}$. Fig. 6(a) shows the output power of PV panel (P_{pv}). At $t = 1$ s, the irradiance is suddenly decreased to 260 W/m². At this irradiance, the PV panel supplies 250 W, but the load demand (P_o) is 480 W. Therefore, V_o is decreased to 34V from 48 V when the PV system is acting alone, i.e. without ESS as shown in Fig. 6(b). To maintain the V_o at 48 V the surplus demand of 230 W (480 - 250) is to be supplied by ESS. Fig. 6(c) shows the battery and SC currents. SC supplies high frequency component (IHFC) of surplus power momentarily, whereas battery supplies the steady state component or low frequency component (ILFC) as shown in Fig. 6(c). As the battery is discharging the SOC is continuously decreasing as shown in Fig. 6(d). At $t = 22$ s the battery reaches SOC_{min} , therefore $SOC_{stat} = -1$, but $\text{sign}(I_{HFC_ref}) = +1$. It means that the voltage control loop is commanding the converter to discharge the current, but battery does not have enough energy as it reaches the lower limit. Therefore, from $I_{HFC_ref} = I_{tot_ref}$ i.e. the total current is to be supplied by SC to maintain the output voltage at 48 V. From the Fig. 6(c), it is observed that SC is discharging the total current, whereas the battery is oscillating around 0 A. Hence the SOC of battery is maintained at SOC_{min} as shown in Fig. 6(d), while maintaining the output voltage at 48 V as shown in Fig.6(b).

B. Case 2: Step Increase in PV Power

In this study, initially the PV panel is operated in maximum power point tracking (MPPT) [14] mode with $S = 520 \text{ W/m}^2$ and $T = 25^\circ\text{C}$. Fig. 7(a) shows the output power of PV panel (P_{pv}). At $t = 1 \text{ s}$, the irradiance is suddenly increased to 780 W/m^2 . At this irradiance, the PV panel supplies 760 W , but the load demand (P_o) is 480 W . Therefore, V_o is increased to 59 V from 48 V when the PV system is acting alone, i.e. without ESS as shown in Fig. 7(b). To maintain the V_o at 48 V the surplus power of 280 W ($760 - 480$) is to be absorbed by ESS. Fig. 7(c) shows the battery and SC currents. SC absorbs IHFC of surplus power momentarily, whereas battery absorbs the steady state component hFC as shown in Fig. 7(c). As the battery is charging the SOC is continuously increasing

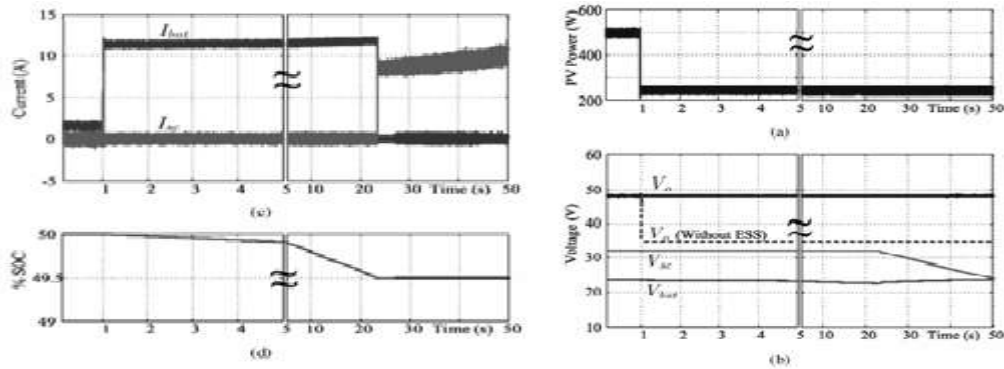


Fig. 6. Simulation results for step decrease in PV generation: a) power, b) Voltage. c) current, and d) SOC of battery shown in Fig. 7(d). At $t = 35 \text{ s}$ the battery reaches SOCmax, therefore SOCstat = +1, but sign(hFC_ref) = -1. It means that the voltage control loop is commanding the converter to charge the current, but battery does not have enough space as it reaches the upper limit. Therefore, from $I_{HFC} = I_{to} \cdot C_{ref}$ i.e. the total current is to be absorbed by SC to maintain the output voltage at 48 V . From the Fig. 7(c), it is observed that SC is charging the total current, whereas the battery is oscillating around 0 A . Hence the SOC of battery is maintained at SOCmax as shown in Fig. 7(d), while maintaining the output voltage at 48 V as shown in Fig. 7(b).

C. Case 3: Step Decrease in Load Demand

In this study, initially the PV panel is operated in maximum power point tracking (MPPT) mode with $S = 520 \text{ W/m}^2$, $T = 25^\circ\text{C}$ and $R = 4.8 \text{ n}$. At $t = 1 \text{ s}$, the load demand is suddenly decreased by increasing R to 7.2 n . Fig. 8(a) shows

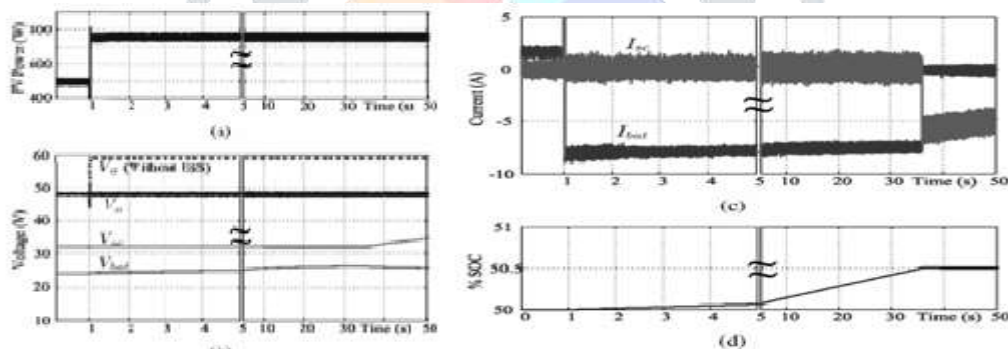


Fig. 7. Simulation results for step increase in PV generation: a) power, b) voltage, C) current, and d) SOC of battery. the load demand (P_o). At this instant, the PV panel supplies 480 W , but the load demand (P_o) is 320 W . Therefore, V_o is increased to 59 V from 48 V when the PV system is acting alone, i.e. without ESS as shown in Fig. 8(b). To maintain the V_o at 48 V the surplus supply of 160 W ($480 - 320$) is to be absorbed by ESS. Fig. 8(c) shows the battery and SC currents. SC absorbs IHFC of surplus power momentarily, whereas battery absorbs the steady state component hFC as shown in Fig. 8(c). As the battery is charging the SOC is continuously increasing as shown in Fig. 8(d). At $t = 47 \text{ s}$ the battery reaches SOCmax, therefore SOCstat = +1, but sign(hFC_ref) = -1. It means that the voltage control loop is commanding the converter to charge the current, but battery does not have enough space as it reaches the upper limit. Therefore, from $I_{HFC} = I_{to} \cdot C_{ref}$ i.e. the total current is to be absorbed by SC to maintain the output voltage at 48 V . From the Fig. 8(c), it is observed that SC is charging the total current, whereas the battery is oscillating around 0 A . Hence the SOC of battery is maintained at SOCmax as shown in Fig. 8(d), while maintaining the output voltage at 48 V as shown in Fig.

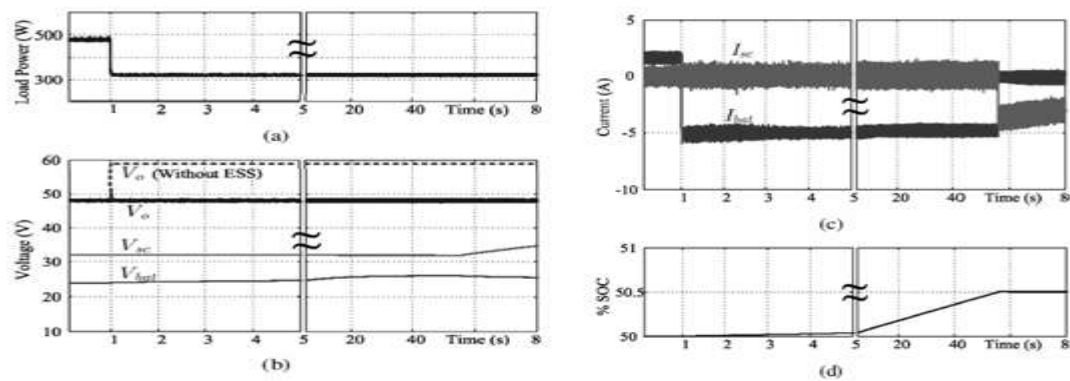


Fig. 8. Simulation results for step decrease in load demand: a) power, b) voltage, c) current, and d) SOC of battery.

D. Case 4: Step Increase in Load Demand

In this study, initially the PV panel is operated in maximum power point tracking (MPPT) mode with $S = 520 \text{ W/m}^2$, $T = 25^\circ\text{C}$ and $R = 4.8 \text{ n}$. At $t = 1 \text{ s}$, the load demand is suddenly increased by decreasing R to 2.4 n . Fig. 9(a) shows the load demand (P_o). At this instant, the PV panel supplies 480 W , but the load demand (P_o) is 960 W . Therefore, V_o is decreased to 34 V from 48 V when the PV system is acting alone, i.e. without ESS as shown in Fig. 9(b). To maintain the V_o at 48 V the surplus demand of 480 W ($960 - 480$) is to be supplied by ESS. Fig. 9(c) shows the battery and SC currents. SC supplies IHFc of surplus power momentarily, whereas battery supplies the steady state component hFC as shown in Fig. 9(c).

As the battery is discharging the SOC is continuously decreasing as shown in Fig. 9(d). At $t = 12 \text{ s}$ the battery reaches SOC_{min}, therefore SOC_{stat} = -1, but sign(hFC_{ref}) = +1. It means that the voltage control loop is commanding the converter to discharge the current, but battery does not have enough power as it reaches the lower limit.

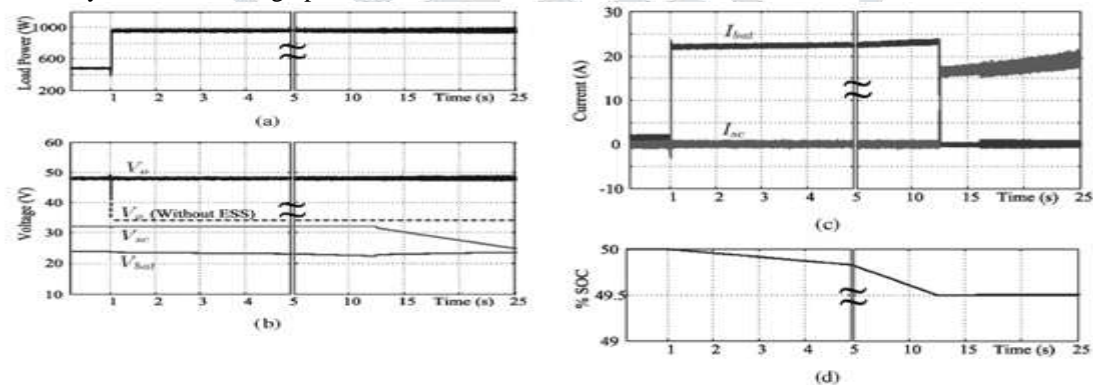


Fig. 9. Simulation results for step increase in load demand: a) power, b) voltage, c) current, and d) SOC of battery.

Therefore, from $I_{HFCref} = I_{ouef}$ i.e. the total current is to be supplied by SC to maintain the output voltage at 48 V . From the Fig. 9(c), it is observed that SC is discharging the total current, whereas the battery is oscillating around 0 A . Hence the SOC of battery is maintained at SOC_{max} as shown in Fig. 9(d), while maintaining the output voltage at 48 V as shown in Fig. 9(b).

V. CONCLUSION

The analysis and design of a novel control strategy for voltage regulation, SOC regulation, and power sharing between battery and SC has been successfully demonstrated through the MATLAB / SIMULINK simulation in this paper. The proposed method is based on decoupling of low and high frequency power components of demand-generation mismatch and utilizes SOC of battery to control battery and Sc. During sudden changes in PV generation and/or load demand, the low frequency power component or steady state component was managed by battery storage system, while the high frequency component was managed by Sc. Hence, stress on battery is reduced and life span increases. Similarly, during the SOC limit violation the charging/discharging currents are diverted to Sc. The proposed algorithm has both the advantages of DC voltage regulation and battery SOC regulation.

REFERENCES

- [1] A. M. Gee, F. V. P. Robinson, and R. W. Dunn, "Analysis of battery lifetime extension in a small-scale wind-energy system using supercapacitors," *IEEE Trans. Energy Convers.*, vol. 28, no. 1, pp. 24-33, Mar. 2013.
- [2] R. Karki and Billinton, "Reliability/cost implications of pv and wind energy utilization in small isolated power systems," *IEEE Trans. Energy Convers.*, vol. 16, no. 4, pp. 368-373, Dec. 2001.
- [3] N. Mendis, K. M. Muttaqi, and S. Perera, "Active power management of a supercapacitor-battery hybrid energy storage system for standalone operation of dfig based wind turbines," in *Proc. 2012 IEEE Industry Applications Society Annual Meeting (IAS)*, pp. 1-8.
- [4] W. Kellogg, M. H. Nehrir, G. Venkataramanan, and V. Gerez, "Generation unit sizing and cost analysis for stand-alone wind, photovoltaic, and hybrid wind/pv systems," *IEEE Trans. Energy Convers.*, vol. 13, no. 1, pp. 70-75, Mar. 1998.

- [5] M. Glavin, P. Chan, S. Armstrong, and W. Hurley, "A stand-alone photovoltaic supercapacitor battery hybrid energy storage system," in Proc. 2008 13th IEEE Power Electronics and Motion Control Conference, p. 1688-1695.
- [6] H. Zhou, T. Bhattacharya, D. Tran, T. Siew, and A. Khambadkone, "Composite energy storage system involving battery and ultracapacitor with dynamic energy management in microgrid applications," IEEE Trans. on Power Electron, vol. 26, no. 3, pp. 923-930, Mar. 2011.
- [7] R. Sathish kumar, K. Sathish Kumar, and M. K. Mishra, "Dynamic energy management of micro grids using battery super capacitor combined storage," in Proc. 2012 Annual IEEE India Conference (INDICON), 2012, pp. 1078-1083.
- [8] Z. Guoju, T. Xi sheng, and Q. Zhiping, "Research on battery supercapacitor hybrid storage and its application in microgrid," in Proc. 2010 IEEE Power and Energy Engineering Conference, pp. 1-4.
- [9] T. Christen and M. W. Carlen, "Theory of ragone plots," Journal of Power Sources, vol. 91, no. 2, pp. 210 - 216, 2000. [Online]. Available: <http://www.sciencedirect.com/science/article/pii/S0378775300004742>
- [10] S. Vazquez, S. M. Lukic, E. Galvan, L. G. Franquelo, and J. M. Carrasco, "Energy storage systems for transport and grid applications," IEEE Trans. Ind. Electron, vol. 57, no. 12, pp. 3881-3895, Dec. 2010.
- [11] W. Li and G. Joos, "A power electronic interface for a battery supercapacitor hybrid energy storage system for wind applications," in Proc. 2008 IEEE Power Electronics Specialists Conference, pp. 1-4.
- [12] A. Lahyani, P. Venet, A. Guermazi, and A. Troudi, "Battery/ supercapacitors combination in uninterruptible power supply (ups)," IEEE Trans. Power Electron, vol. 28, no. 4, pp. 1509-1522, Apr. 2013.
- [13] L. Wei, G. Joos, and B. L. , "Real-time simulation of a wind turbine generator coupled with a battery supercapacitor energy storage system," IEEE Trans. Power Electron, vol. 57, no. 4, pp. 1137-1145, Apr. 2010.
- [14] Y T. Tan, D. Kirschen, and N. Jenkins, "A model of pv generation suitable for stability analysis," IEEE Trans. Energy Convers., vol. 19, no. 4, pp. 748 - 755, Dec. 2004.
- [15] H.-L. Tsai, c.-S. Tu, and Y.-J. Su, "Development of generalized photovoltaic model using matlab/simulink," in Proc. 2008 the World Congress on Engineering and Computer Science, pp. 846-851.

